



Assessment and Improvement of a Novel ultrasound-based 3D Reconstruction Method: Registered for Lumbar Spine

Mohammad Reza Effatparvar^{1,2,3} · Marc-Olivier St. Pierre^{1,2,3} · Stéphane Sobczak^{1,2,3}

Received: 29 September 2022 / Accepted: 2 November 2022 / Published online: 16 November 2022
© Taiwanese Society of Biomedical Engineering 2022

Abstract

Purpose Bone three-dimensional (3D) modelling using imaging techniques is applied for 3D kinematic measurement. Ultrasound has been recently introduced for 3D bone modelling. This study intends to assess and improves an ultrasound-based 3D modelling algorithm to a soft tissue-compatible version.

Methods Six lumbar spines with attached soft tissues were dissected from human cadavers with different body mass indexes (BMIs). Ultrasound and computed tomography (CT) scan imaging were performed, and the images were reconstructed three-dimensionally using image processing techniques. Regarding reliability, an operator repeated the reconstruction processes of two specimens three times. Regarding validity, 3D models were directly compared; then, volumes were calculated, and limits of agreement were obtained. Finally, the fat pad thickness of all spinous processes was measured to calculate the effect of different BMIs on reconstruction errors.

Results The reliability analysis using intraclass correlation coefficients [95% CI] showed high intra-operator reliability in the CT-scan- (0.966 ± 0.014) and ultrasound-based (0.930 ± 0.012) models. The low mean mean reconstruction errors (mm) (0.18 ± 0.04, 0.24 ± 0.11, 0.06 ± 0.15, 0.04 ± 0.36, 0.44 ± 0.24, and 0.42 ± 0.27, respectively from specimen 1 to 6), And also the inclusion of all differences within the limit of agreement verified the validity of ultrasound-based models compared to CT-scan-based models. Moreover, the linear regression showed a weak correlation ($R = 0.33$) between the reconstruction error and fat pad thickness.

Conclusion This study showed that the 3D reconstruction of the lumbar spine obtained from ultrasound images is highly similar to those obtained from CT scan images and is not significantly affected by the posterior fat pad, which makes it appropriate for kinematic studies.

Keywords Lumbar spine · Ultrasound · CT scan · Kinematic · 3D spine modelling

1 Introduction

Three-dimensional (3D) bone reconstruction using medical imaging as one of the most effective modelling methods is used for different purposes such as mechanical tests, surgical

preplanning, and kinematic study. Magnetic resonance imaging (MRI) [1] and computed tomography (CT) scan [2] are the leading imaging systems for creating 3D models. However, the introduced approaches have many disadvantages; X-ray imaging is ionizing and deleterious for the body tissue. MRI is very expensive and imposes a high cost on the health system. Hence, employing an alternative imaging method with the lesser drawbacks is crucial.

Meanwhile, ultrasound imaging as an affordable, portable, and non-ionizing modality can fill the available gap. Although in the opinion of many researchers, this imaging method still faces many limitations, validation results of the ultrasound images compared to other methods like comparison with CT scan in aortic aneurysm diameter measurements with a measurement error of 0.11 ± 4.26 mm [3], comparison with MRI-CT images of a beating heart phantom with

✉ Mohammad Reza Effatparvar
Mohammad.reza.ffmpeg@uqtr.ca

¹ Chaire de Recherche en Anatomie Fonctionnelle, Université du Québec à Trois-Rivières, 3351, boulevard des Forges, Trois-Rivières, Québec G8Z 4M3, Canada

² Département d'anatomie, Université du Québec à Trois-Rivières, Trois-Rivières, Québec, Canada

³ Groupe de Recherche sur les Affections Neuromusculosquelettiques, Université du Québec à Trois-Rivières, Trois-Rivières, Québec, Canada

a measurement error of 1.7 ± 0.4 mm [4], comparison with a caliper in spine height measurement with a measurement error of $5.5 \pm 1.5\%$ [5], and recent innovative developments have made it replaceable with other imaging systems in certain situations. As an example, several intra-operative applications like fracture reduction [6], arthroscopic surgeries [7], screw insertion, anatomical bone landmark determination, tumour border delineation [8], and point-of-care applications like bone fractures identification [9–11], spinal cord injuries diagnosis [12] could be mentioned.

In addition, ultrasound images have been recently used for bone 3D reconstruction to make the less intelligible images highly acceptable. Newly, many applications of ultrasound-based bone 3D modelling have been reported, such as the modelling of the knee joint for robotic knee arthroplasty [13], co-applying of the ultrasound imaging system and the electromagnetic tracker for the knee 3D reconstruction [14], and co-registering the ultrasound with CT scan images to model cow femur [15]. Moreover, various methods of spine 3D modelling have been applied in order to measure spinal rotation, scoliosis, and other deformities using a 3D ultrasound machine [16–19].

Nevertheless, among the ultrasound applications, less attention has been paid to the issue of spine kinematics measurement, and the existing studies have been limited to two-dimensional measurements [20]. While spine kinematics, as an essential criterion in movement limitation examination, should be analysed three-dimensionally. On the other hand, since the spine 3D models could be used to localize bone landmarks to determine spine kinematics, we decided to study the possibility of 3D reconstruction of the lumbar spine through ultrasound images. In this regard, we aimed to assess and develop an available algorithm of one dry lumbar spine 3D reconstruction [21] to a more substantial version by reconstructing complete lumbar spines (T12-S1) with soft tissues and different fat pad thicknesses, so linked to the body mass indexes (BMIs). Thanks to valid 3D bone models from ultrasound we will be able to determine in vivo lumbar spine kinematics in a near future.

2 Materials and Methods

2.1 Specimen

After attaining approval from the Université du Québec à Trois-Rivières Institutional Review Board (SCELERA 21–13), Six human cadavers with different BMIs ranged from 18 to 26 (Mean: 21.8, SD: ± 3.3) and ages from 62 to 89 years (Mean: 76.3 SD: ± 10) were dissected to extract the lumbar spines from T12 to S2. During the dissections process, First, palpating the spinous processes, two longitudinal incisions were made 15 to 20 cm laterally away from the spinous

processes to leave an adequate amount of soft tissue covering the lumbar spine posteriorly. Then, dissections were continued obliquely up to the anterior side of the vertebral body to keep all the attached lateral soft tissues intact. Next, the edges of the skins were sutured to get a cylindrical form, and two orthopaedic Schanz screws were inserted through all vertebral bodies to avoid inter vertebral displacement (Fig. 1a). Then, the Schanz screws were fixed on a threaded rod using external fixation clamps. Following, each specimen was installed in the centre of a home-made cylinder plastic frame (D = 165 mm), and the frame was filled up with porcine gelatine (Gelatine, Type A, Pork Skin, mi. Bloom 225) (Fig. 1b).

2.2 CT Scan

After gelatine hardening, a CT scan device (GE Healthcare, Revolution EVO) was used to collect the images of the specimens. In this regard, after setting up the CT scan machine (convolution Kernel = standard, filter type = body filter, window centre = 50, window width = 500, focal spot = 1.2 mm) the DICOM format images (reconstruction slice thickness = 0.5 mm, inter-slice spacing = 0.625 mm, each image size = 514 KB) were obtained.

2.3 Ultrasound

After CT scan imaging, the specimens were stabilized into a computer-assisted mechanical frame (CAM) [21], facilitating whole-length ultrasonography. The CAM (Fig. 2) provides a graduated circular mobile plate that moves upward and downward at the desired speed, controlled by a step motor. Moreover, this mobile plate contains a holder for the ultrasound transducer, which could be set at the desired degree. Through these facilities, ultrasound collects the images from down to up at each upward movement of the mobile plate. Then, the transducer holder is moved in the circular path to the next position, and the imaging is repeated; this process is continued until finishing imaging all around the spine. For this study, the imaging processes were performed using a linear transducer of an ultrasound machine (NextGen LOGIQ e Ultrasound, GE Healthcare, USA - Mode = Musculoskeletal, Frequency = 8.0 MHz, Distance = 8 cm, Gain = 76). Furthermore, the CAM setup was at 0.5 mm/s of linear velocity (upward-downward) and every 30 to 40 degrees (circular path). These degrees were calculated using the Eq. (1) and depending on the circumferences of the specimens; to be fully covered in the images with the fewest overlap, preventing shadows.

$$\theta \cong \frac{360T}{2\pi r} \quad (1)$$

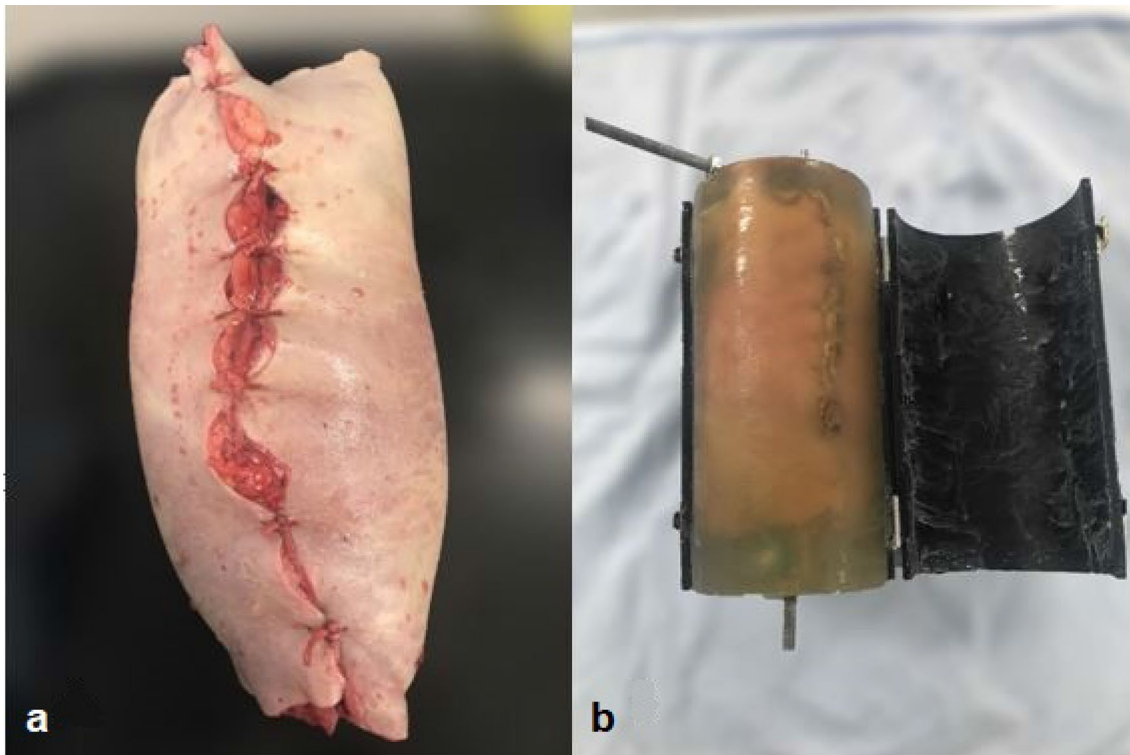


Fig. 1 (a) a dissected lumbar spine after suture. (b) a specimen fixed in the gelatine after hardening

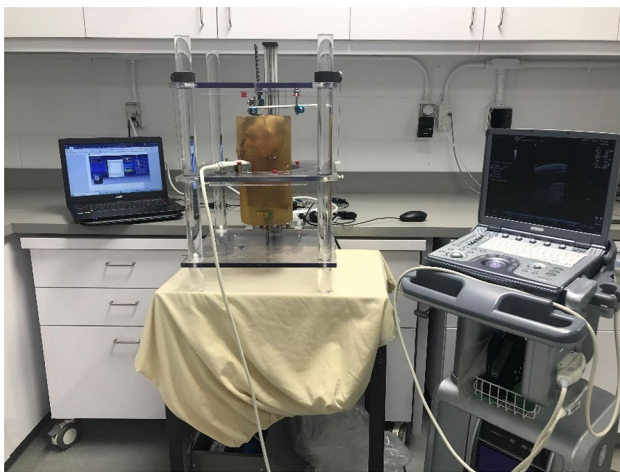


Fig. 2 The procedure of ultrasound imaging using CAM.

In this equation, “ θ ” is the degree setup of the mobile plate, “ T ” is the transducer width and “ 2π ” is the circumference of the specimen.

2.4 Image Processing and 3D Reconstruction

After finishing the ultrasound imaging process, 9 to 12 ($360/\theta$) sets of ultrasound files, including 400 DICOM

format images (each image size = 22.2 KB), were obtained. Then, using a homemade MATLAB software (MathWorks, R2021 a) script, the sets of images were merged to produce one series of 360-degree DICOM format images (image amount = 400). Next, to simplify the reconstruction process, the quality of images was enhanced using intensity transform, Laplacian spatial filter, high pass filter, and colour thresholds (Fig. 3).

In the following step, using the segmentation tool of Amira software (5.2.2®, Germany), the images obtained from the ultrasound and the CT scan (gold standard) were separately segmented to create 3D models (Fig. 4).

2.5 Comparison and Measurement

2.5.1 Reliability Procedure

The segmentation processes of the ultrasound images and CT scan images belonging to the first and second specimens were each repeated three times by the same operator. Then, using CloudCompare software (v2.12 Beta, France) all vertebrae were separated, the volumes were determined and compared to measure the intra-operator reliability of 3D reconstruction. To separate the vertebrae, since the articular processes were not easily separable between two vertebrae in ultrasound-based 3D models because of the limitations,

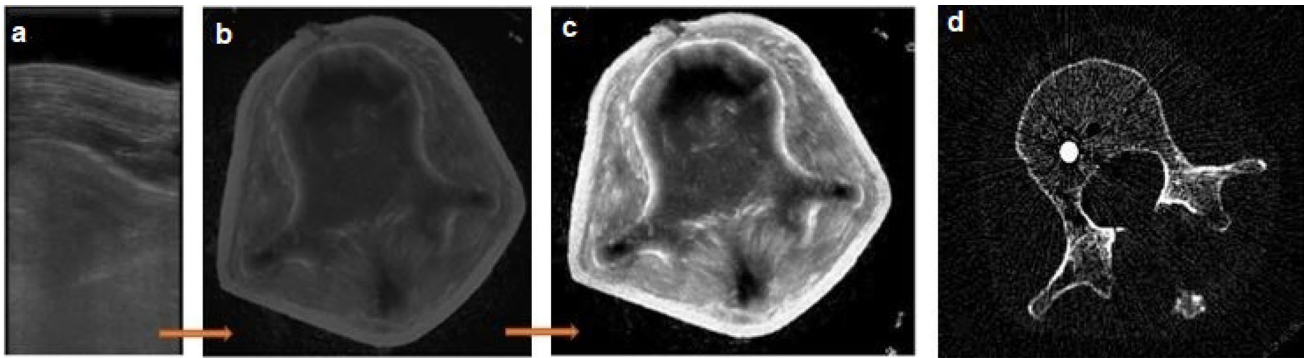


Fig. 3 (a) one of the obtained images from ultrasound. (b) a 360-degree image after merging process. (c) a quality enhanced image after image processing. (d) intensity boundaries changed CT scan image of the same level

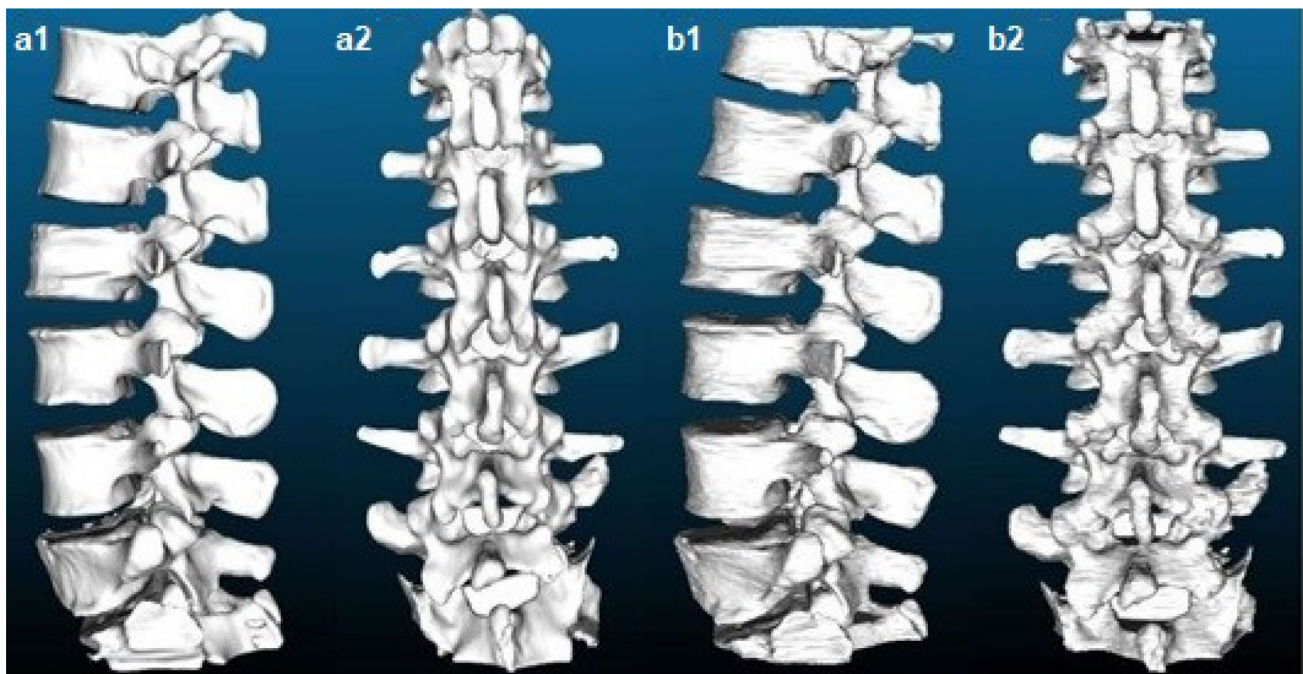


Fig. 4 The lateral view (a1) and the posterior view (a2) of a CT-scan-based 3D model. the lateral view (b1) and the posterior view (b2) of an ultrasound-based 3D model from one specimen

first CT-scan-based and ultrasound-based 3D models were aligned by picking equivalent point pairs. Then, the vertebrae in the ultrasound-based models were separated using the pattern created through the CT-scan-based models. After separating the vertebrae, the volume of each were determined.

2.5.2 Validation Process

After reconstructions, two validation steps were applied. Concerning the first step, using CloudCompare [22], ultrasound-based models were directly compared to the CT-scan-based models as the gold standard; in this step,

all vertebrae were separated and compared one by one. In this comparison, the distances are computed based on the nearest neighbour distance technique. It means that the software selects a point on the reference model (CT scan), then searches for the nearest point on the compared model (ultrasound), measures the direct distance (mm), and finally reports the mean of all point-to-point (mesh-to-mesh) distances as the reconstruction error. In addition, colour maps were provided in the comparison images to highlight the differences between the two models graphically.

Then, in the second step, using the same software, the volume of each vertebra was computed, the mean volumes

of vertebrae were compared and the agreement between the two modelling techniques were analysed.

2.5.3 Correlation Measurement

Since posterior elements are the most important part of 3D reconstructions to be used in kinematic studies, the thickness of the fat pad between the skin and spinous process was considered a criterion and was measured using CT scan images. For this measurement, the image slides in which spinous processes were in the maximum length were used. Then, the correlation of the fat pad with reconstruction errors was calculated to see the effect of the fat pad on ultrasound-based 3D reconstructions.

2.6 Statistical Analysis

In order to assess the intra-operator reliability, intraclass correlations coefficient (ICC – 2.1 Two-Way random) on volumes measured on CT-scan- and ultrasound-based 3D bone reconstructions with 95% CI were calculated.

Regarding the second step of validation, since the specimens are considered as whole samples, the limits of agreement between CT-scan- and ultrasound-based models were calculated and Bland-Altman plots were reported. Finally, the linear regression was graphed to calculate the correlation between reconstruction error and fat pad thickness. All statistical analysis was performed using SPSS software

(SPSS Statistics 236 for Windows, version 28.0; IBM Corp., Armonk, NY, 237 USA).

3 Results

Concerning the intra-operator reliability, the intraclass correlations coefficients [95% CI] between different times of reconstructions were calculated (Table 1), and the mean intra-operator reliabilities for the CT-scan-based and the ultrasound-based models were 0.966 ± 0.014 and 0.930 ± 0.012 , respectively.

Concerning the verification of the validity of the ultrasound-based 3D models, first, they were directly compared with the CT-scan-based 3D models as a gold standard. In this comparison, the mean mean reconstruction errors (mm) by specimen were: 0.18 ± 0.04 for specimen 1, 0.24 ± 0.11 for specimen 2, 0.06 ± 0.15 for specimen 3, 0.04 ± 0.36 for specimen 4, 0.44 ± 0.24 for specimen 5 and 0.42 ± 0.27 for specimen 6. Moreover, the mean mean reconstruction errors (mm) by vertebra were: 0.23 ± 0.12 for L1, 0.15 ± 0.39 for L2, 0.3 ± 0.31 for L3, 0.31 ± 0.29 for L4 and 0.15 ± 0.05 for L5. The reconstruction errors of each specimen and vertebra are reported in Table 2.

Also, the graphical models indicating colormaps in the range of -1 to 1 mm were extracted to demonstrate the comparisons (Fig. 5). one specimen's figures are presented here due to space limitations.

In addition, as the second validation step, the volume of each vertebra was calculated in two methods separately; the mean mean volume of all vertebrae for the CT-scan-based 3D models was 55788.8 ± 1942.32 mm³ with a coefficient of variation of 3.48% and standard error of 868.63 mm³ and for the ultrasound-based 3D models was 56790.5 ± 2100.71 mm³ with a coefficient of variation of 3.69% and standard error of 939.46 mm³. The mean values are presented in Table 3. Then, considering specimens as whole samples, limits of agreement ($95\% \pm 1.96$ Sd) (Table 4) and the Bland-Altman plot (Fig. 6) between the two reconstruction

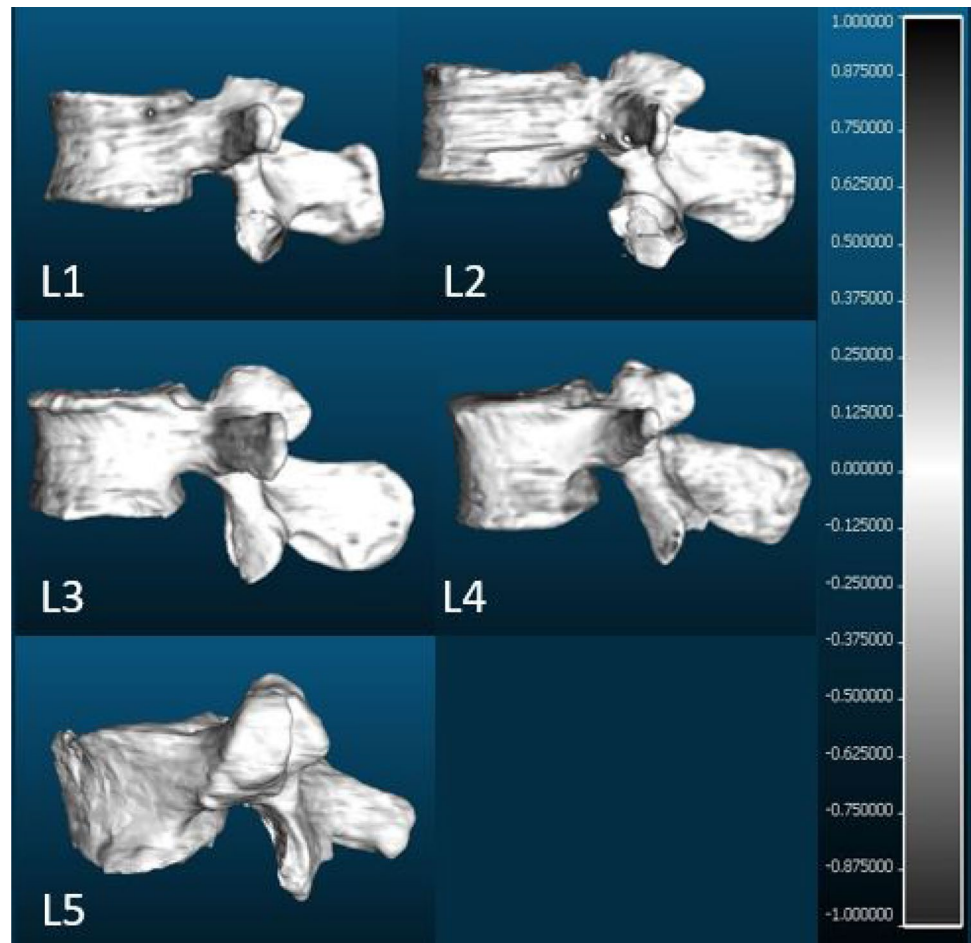
Table 1 Intra-operator intraclass correlation coefficient [95% CI]

	Intra-operator	
	CT-scan-based model	Ultrasound-based model
Specimen 1	0.977 [0.898 – 0.997]	0.939 [0.408 – 0.994]
Specimen 2	0.956 [0.803 – 0.995]	0.922 [0.584 – 0.991]
Mean	0.966	0.930
SD	0.014	0.012

Table 2 Reconstruction errors (mm) between the ultrasound-based and the CT-scan-based models. In this table, SP stands for specimen and L stands for Lumbar vertebra. The negative errors mean the compared models (ultrasound) have lower values

	SP1 Mean error (BMI \approx 18)	SP2 Mean error (BMI \approx 19)	SP3 Mean error (BMI \approx 20)	SP4 Mean error (BMI \approx 23)	SP5 Mean error (BMI \approx 25)	SP6 Mean error (BMI \approx 26)	Mean mean error
L1	0.1 ± 0.6	0.4 ± 1.2	0.1 ± 0.7	0.2 ± 1.1	0.3 ± 0.4	0.3 ± 0.8	0.23 ± 0.12
L2	0.2 ± 0.5	0.2 ± 0.7	0.2 ± 0.5	-0.6 ± 0.4	0.6 ± 0.6	0.3 ± 0.7	0.15 ± 0.39
L3	0.2 ± 0.6	0.1 ± 0.9	-0.1 ± 0.4	0.3 ± 0.2	0.5 ± 0.6	0.8 ± 0.4	0.3 ± 0.31
L4	0.2 ± 0.5	0.3 ± 0.8	-0.1 ± 0.5	0.2 ± 0.3	0.7 ± 0.5	0.6 ± 0.3	0.31 ± 0.29
L5	0.2 ± 0.5	0.2 ± 0.9	0.2 ± 0.6	0.1 ± 0.3	0.1 ± 0.8	0.1 ± 0.6	0.15 ± 0.05
Mean mean error	0.18 ± 0.04	0.24 ± 0.11	0.06 ± 0.15	0.04 ± 0.36	0.44 ± 0.24	0.42 ± 0.27	

Fig. 5 Lateral views of 3D reconstructions comparative images from one specimen



techniques were obtained. The mean mean difference was $1001.7 \pm 683.16 \text{ mm}^3$.

Concerning the correlation between the reconstruction error and the fat pad thickness (Table 5), the linear regression (Fig. 7) showed a correlation of $R = 0.33$.

4 Discussion

Measuring spine kinematics is essential to analyse and diagnose the spine's movement abnormalities, such as hypermobility or hypo-mobility. Today, several methods are used to measure spine kinematics; meanwhile, clinically, it has been limited to a physical examination. Still, for 3D measurement, the method of localizing bone landmarks on the spine 3D model has been developed recently. Concerning obtaining 3D models of the spine, two imaging modalities are mostly used: CT scan and MRI. Yet, these modalities have disadvantages as previously mentioned.

In the meantime, the ultrasound machine could act as an alternative. Therefore, the primary purpose of this study was to improve an algorithm for imaging the spine using ultrasound and converting the obtained images into 3D models.

For this purpose, since an innovative technique for 3D reconstruction of a dry vertebra has been recently introduced with significant accuracy and precision [21], in this study, we tried to assess and improve this technique in the 3D reconstruction of six lumbar spines with different BMIs and fat pad thicknesses. So, in this regard, the imaging operations were experimentally performed in certain degrees, definable by Eq. (1), to cover the entire specimen and reduce the shadow. Then, since the vertebrae were covered with soft tissue, the image processing techniques were applied to enhance the quality of images and facilitate the segmentation process (Fig. 3).

After finishing the 3D reconstruction processes, two steps were introduced to verify the validity of the ultrasound-based 3D models compared to the CT-scan-based 3D models (gold standard). In the first step, using CloudCompare, all vertebrae of each specimen were separated and compared one by one. In this regard, the mean mean reconstruction errors reported in Table 2 show that, globally, there are a slight overestimation for the ultrasound-based 3D models compared to the CT-scan-based 3D models. However, although there are overestimations for the ultrasound-based models, low variations between the reconstructions

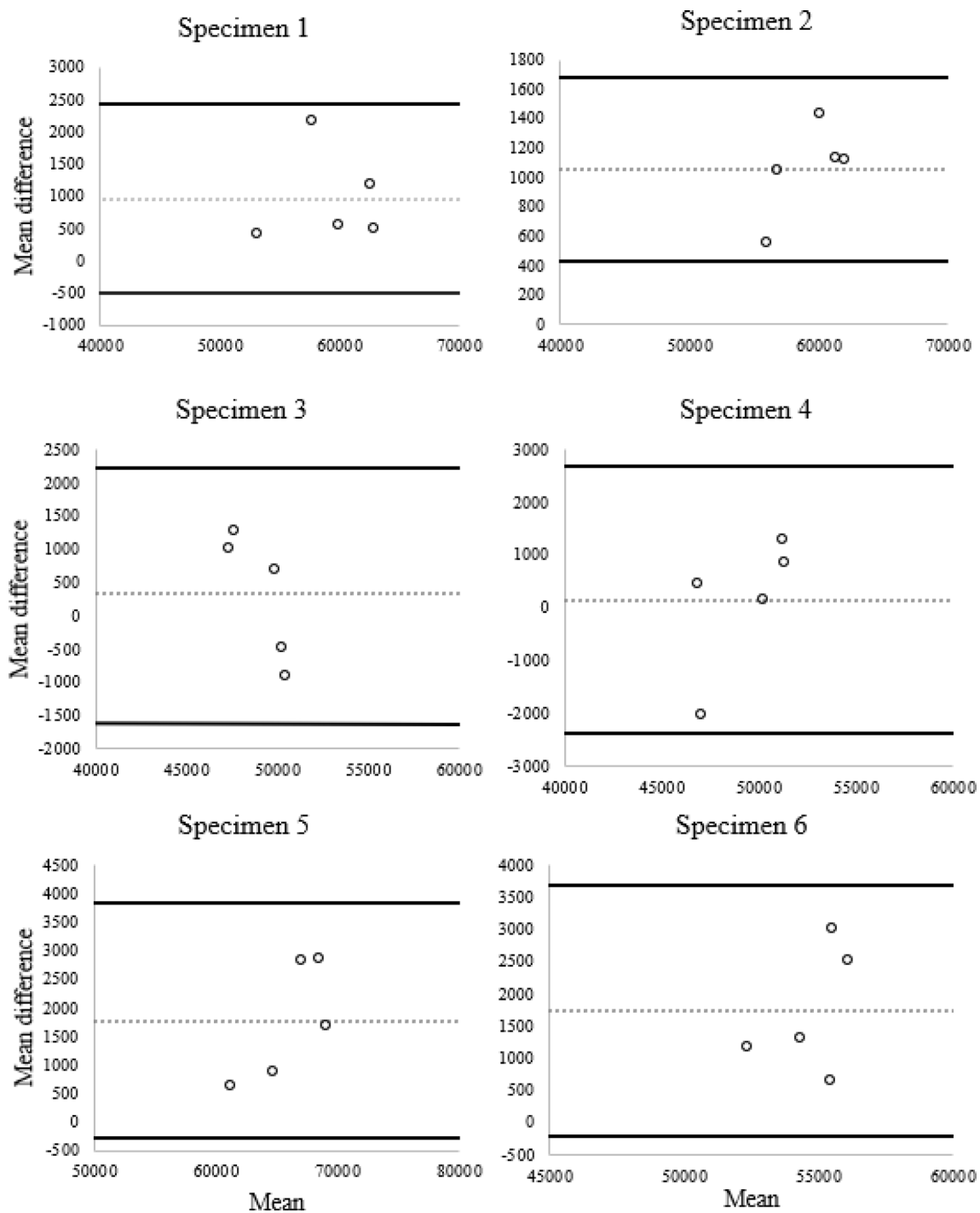


Fig. 6 Bland and Altman plots: comparisons between ultrasound-based 3D models and CT-scan-based 3D models. Dotted lines represent the mean differences and continuous lines represent the upper and lower limits of agreement. Values are reported in Table 3

regarding the vertebrae sizes demonstrate the high validity of the models obtained from ultrasound. Moreover, the overestimated results in this research, in addition to being similar to the previous study [21] which was 0.44 ± 0.63 mm, have also been observed in other ultrasound-Ct scan comparative studies, like in measuring kidney stone size with an average

overestimation of 3.8 ± 2.4 mm [23], and measuring aortic aneurysm diameter with an average overestimation of 0.11 ± 4.26 mm [3].

In addition, the graphical models (Fig. 5) with the related colour map in the range of -1 to 1 mm were extracted to show the differences between the two methods of

reconstructions. Since in these graphical models, the vertebrae were coloured in white, and the errors in each area were changed from white at zero to black at - 1 and 1 mm, the slight colour change in the comparative image indicates the high accuracy of ultrasound models.

Concerning the second validation step, the volumes of all vertebrae in the ultrasound- and CT-scan-based 3D models were computed and compared. Since the first validation step showed overestimations in linear distance between ultrasound-and CT-scan-based 3D models, larger volumes for ultrasound-based 3D models are expectable. Therefore, based on the reported values in Table 3, the vertebrae of the ultrasound-based 3D models have higher volumes than the CT-scan-based 3D models, although the differences are insignificant considering the amounts of volumes. Also, the CVs of mean volumes coming from the same table showed the low variability of measurement for both ultrasound-based and CT-scan-based methods. In addition, considering all specimens as whole samples, the limits of agreement were calculated and plotted using the Bland-Altman method. As observed in Fig. 6, all differences were included within the limit of agreement, which indicates that the results obtained from ultrasound compared to CT scan are valid.

Concerning the intra-operator reliability, a high degree of reliability was observed between the different reconstruction times of CT-scan (0.966 ± 0.014) and ultrasound images (0.930 ± 0.012). These reliability results are similar to the previous studies [5, 21, 24–26] and showed a high consistency for the current reconstruction algorithm.

On the other hand, one of the main objectives of this study was to investigate the effect of the soft tissue of the lumbar spine on the results of reconstructions. Therefore, the soft tissue in the posterior part of the lumbar spine remained intact. Since fat tissue has the most significant effect on ultrasound, in this study, the amount of fat pad between the spinous processes and the skin was considered a criterion for examining the correlation between the fat

pad thickness and reconstruction error. Based on the linear regression diagram results in Fig. 6, there is a weak correlation ($r = 0.33$) between reconstruction error and the fat pad thickness. Although there have been slightly higher errors for some of the vertebrae, the weak correlation shows that the posterior soft tissues would not significantly affect the reconstructions. Since the posterior elements are the most functional anatomical parts for the kinematic study to locate the landmarks, only posterior soft tissues were kept intact. Otherwise, if the abdominal fat tissue in the anterior part was kept, it could make difficulties in imaging.

Regardless of all numerical data, the delicate appearance of the spinous and costiform processes in the ultrasound-based 3D models would indicate an acceptable ability of this method to be used for kinematic studies and locate bones landmarks.

As limitations of this study, as previously mentioned, the CT-scan-based 3D models were used as a pattern to separate the facet joints of vertebrae in ultrasound-based models. Although this method covers the reconstruction errors in the ultrasound-based models, the limitations are

Table 3 Mean volume, standard deviation (SD), coefficient of variation (%), and standard error (SE) of the mean of the all lumbar vertebrae (L) among all specimens. All values are in mm³

	Mean volumes from the CT-scan-based models	Mean volumes from the ultrasound-based models
L1	53040.05	54043.43
L2	55048.93	55880.85
L3	57810.2	58827.56
L4	57477.68	58981.78
L5	55567.13	56218.86
Mean	55788.8	56790.5
SD	1942.32	2100.71
CV(%)	3.48%	3.69%
SE	868.63	939.46

Table 4 Mean differences (MD), upper and lower limits of agreements ($95\% \pm 1.96$ Sd) for all specimens with overall vertebrae. All values are in mm³

	MD	Limits of agreement	
		Upper	Lower
Specimen 1	966.23	2421.74	489.22
Specimen 2	1058.84	1682.58	435.09
Specimen 3	326.62	2220.91	- 1567.68
Specimen 4	145.6	2682.73	- 489.22
Specimen 5	1780.34	3844.19	- 283.51
Specimen 6	1732.54	3860.61	- 215.53
Mean	1001.7		
SD	683.16		

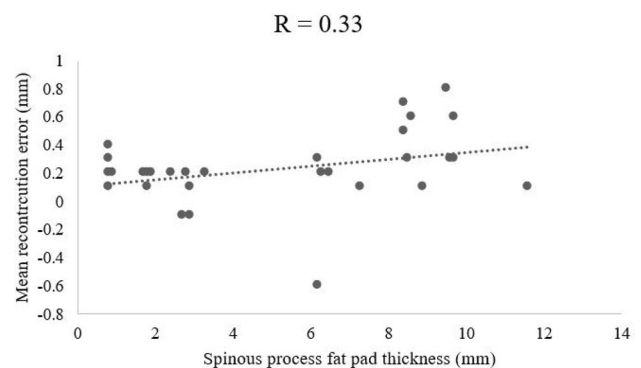


Fig. 7 Linear regression of reconstruction error and spinous process fat pad thickness

Table 5 Fat pad thickness between spinous process and skin. These values were measured in the image slides in which spinous processes were in the maximum length. The letters L stand for Lumbar vertebrae. All values are in mm

	specimen 1	specimen 2	specimen 3	specimen 4	specimen 5	specimen 6
L1	0.8	1.8	2.9	6.3	8.5	9.7
L2	0.9	1.7	2.8	6.2	8.6	9.6
L3	0.8	1.8	2.7	6.2	8.4	9.5
L4	0.8	1.9	2.9	6.5	8.4	9.7
L5	0.8	2.4	3.3	7.3	8.9	11.6

negligible since the articular processes are not considered to be used for the kinematic study. The second limitation of this study was the 3D reconstruction of all around the vertebrae, which is not applicable for in-vivo kinematic study because of the abdominal fat pad and viscera. Still, since the precise localization of three landmarks is required to introduce a coordinate system and accurately measure the kinematic, the complete lumbar spines were used for this in-vitro study.

Regarding the feasibility of this method in clinical measurements, as mentioned in the limitation, although it is not practicable in the current format, the improvement of ultrasound imaging methods and 3D reconstruction of the posterior elements of the lumbar spine will make this method easily achievable for clinical measurement.

In conclusion, this study's results showed that the 3D reconstruction of the lumbar spine obtained from ultrasound images is highly similar to those obtained from CT scan images and is not significantly affected by the posterior fat pad, which makes it appropriate for kinematic studies.

Acknowledgements We thank Collège Lafèche's (Trois-Rivières, Quebec, Canada) radiology department for providing the CT scan system. We would like to give special thanks to all the people who have donated their bodies to science, as well as their families. We are also very grateful to the technicians of the anatomy laboratory where this research was conducted.

Author Contributions All authors contributed to the study conception and design. The first draft of the manuscript was written by Mohammad Reza Effatparvar and all authors commented on previous versions of the manuscript. All authors read and approved the final manuscript.

Funding Author Mohammad Reza Effatparvar has received research support from Fonds de recherche du Québec – Nature et Technologie (FRQNT) under grant [319993]. Author Stephane Sobczak has received research support from Natural Sciences and Engineering Research Council of Canada (NSERC) under grant [RGPIN-2016-05717].

Declarations

Conflict of interest The authors have no relevant financial or non-financial interests to disclose.

Ethical Approval This study was performed in line with the principles of the Declaration of Helsinki. Approval was granted by 'The Ethics Subcommittee of the Anatomy Laboratory for Teaching and Research' of Université du Québec à Trois-Rivières (Date: 2021/10/12-No: SCELERA 21 – 13).

References

- Li, G., Wang, S., Passias, P., Xia, Q., Li, G., & Wood, K. (2009). Segmental in vivo vertebral motion during functional human lumbar spine activities. *European Spine Journal*, 18(7), 1013–1021.
- Vania, M., Mureja, D., & Lee, D. (2019). Automatic spine segmentation from CT images using convolutional neural network via redundant generation of class labels. *Journal of Computational Design and Engineering*, 6(2), 224–232.
- Han, S. M., Patel, K., Rowe, V. L., Perese, S., Bond, A., & Weaver, F. A. (2010). Ultrasound-determined diameter measurements are more accurate than axial computed tomography after endovascular aortic aneurysm repair. *Journal of Vascular Surgery*, 51(6), 1381–1389.
- Huang, X., Moore, J., Guiraudon, G., Jones, D. L., Bainbridge, D., Ren, J., & Peters, T. M. (2009). Dynamic 2D ultrasound and 3D CT image registration of the beating heart. *IEEE Transactions on Medical Imaging*, 28(8), 1179–1189.
- Sobczak, S., Dugailly, P. M., Gilbert, K. K., Hooper, T. L., Sizer Jr, P. S., James, C. R., & Brismée, J. M. (2016). Reliability and validation of in vitro lumbar spine height measurements using musculoskeletal ultrasound: a preliminary investigation. *Journal of Back and Musculoskeletal Rehabilitation*, 29(1), 171–182.
- Wu, Y., Lu, R., Liao, S., Ding, X., Su, W., & Wei, Q. (2021). Application of ultrasound in the closed reduction and percutaneous pinning in supracondylar humeral fractures. *Journal of Orthopaedic Surgery and Research*, 16(1), 1–8.
- Mhaskar, V. A., Agrahari, H., & Maheshwari, J. (2022). Ultrasound guided arthroscopic meniscus surgery. *Journal of Ultrasound*. <https://doi.org/10.1007/s40477-022-00680-5>
- Patel, M. R., Jacob, K. C., Parsons, A. W., Chavez, F. A., Ribot, M. A., Munim, M. A., Vanjani, N. N., Pawlowski, H., Prabhu, M. C., & Singh, K. (2022). Systematic Review: Applications of Intraoperative Ultrasound in Spinal Surgery. *World Neurosurgery*. <https://doi.org/10.1016/j.wneu.2022.02.130>
- Moran, M., & Myers, M. (2022). Use of ultrasonography for identification of long bone fractures. *Visual Journal of Emergency Medicine*, 28, 101381.
- Champagne, N., Eadie, L., Regan, L., & Wilson, P. (2019). The effectiveness of ultrasound in the detection of fractures in adults with suspected upper or lower limb injury: A systematic review and subgroup meta-analysis. *BMC Emergency Medicine*, 19(1), 1–15.
- Qadi, H., Davidson, J., Trauer, M., & Beese, R. (2020). Ultrasound of bone fractures. *Ultrasound*, 28(2), 118–123.
- Vk, V., Bhoi, S., Aggarwal, P., Murmu, L. R., Agrawal, D., Kumar, A., Sinha, T. P., & Galwankar, S. (2021). Diagnostic utility of point of care ultrasound in identifying cervical spine injury in emergency settings. *Australasian Journal of Ultrasound in Medicine*, 24(4), 208–216.
- Kerr, W., Rowe, P., & Pierce, S. G. (2017). Accurate 3D reconstruction of bony surfaces using ultrasonic synthetic aperture techniques for robotic knee arthroplasty. *Computerized Medical Imaging and Graphics*, 58, 23–32.

14. Mahfouz, M. R., Fatah, A., Johnson, E. E., J. M., & Komistek, R. D. (2021). A novel approach to 3D bone creation in minutes: 3D ultrasound. *The Bone & Joint Journal*, *103*(6 Supple A), 81–86.
15. Gonçalves, P. J., & Torres, P. M. (2010). Registration of Bone Ultrasound Images to CT based 3D Bone Models. In *6th International Conference on Technology and Medical Sciences, Porto, Portugal* (pp. 21–23).
16. Vo, Q. N., Le, L. H., & Lou, E. (2019). A semi-automatic 3D ultrasound reconstruction method to assess the true severity of adolescent idiopathic scoliosis. *Medical & Biological Engineering & Computing*, *57*(10), 2115–2128.
17. Vo, Q. N., Lou, E. H., & Le, L. H. (2015). Measurement of axial vertebral rotation using three-dimensional ultrasound images. *Scoliosis*, *10*(2), 1–4.
18. Vo, Q. N., Lou, E. H., & Le, L. H. (2015). 3D ultrasound imaging method to assess the true spinal deformity. In *2015 37th Annual International Conference of the IEEE Engineering in Medicine and Biology Society (EMBC)* (pp. 1540–1543). IEEE.
19. Nguyen, D. V., Vo, Q. N., Le, L. H., & Lou, E. H. (2015). Validation of 3D surface reconstruction of vertebrae and spinal column using 3D ultrasound data—A pilot study. *Medical Engineering & Physics*, *37*(2), 239–244.
20. Effatparvar, M. R., & Sobczak, S. (2022). Application of ultrasound in spine kinematic determination: A systemic review. *Journal of Medical Ultrasound*, *30*(1), 6.
21. Forbes, A., Cantin, V., Develle, Y., Dubé, Y., Bertrand-Grenier, A., Ménard-Lebel, C., & Sobczak, S. (2021). Musculoskeletal ultrasound for 3D bone modeling: A preliminary study applied to lumbar vertebra. *Journal of Back and Musculoskeletal Rehabilitation*, *34*(6), 937–950.
22. Fournier, G., Savall, F., Galibourg, A., Gély, L., Telmon, N., & Maret, D. (2020). Three-dimensional analysis of bitemarks: A validation study using an intraoral scanner. *Forensic Science International*, *309*, 110198.
23. Dai, J. C., Dunmire, B., Sternberg, K. M., Liu, Z., Larson, T., Thiel, J., Chang, H. C., Harper, J. D., Bailey, M. R., & Sorensen, M. D. (2018). Retrospective comparison of measured stone size and posterior acoustic shadow width in clinical ultrasound images. *World Journal of Urology*, *36*(5), 727–732.
24. Zheng, Y. P., Lee, T. T. Y., Lai, K. K. L., Yip, B. H. K., Zhou, G. Q., Jiang, W. W., Cheung, J. C., Wong, M. S., Ng, B. K., Cheng, J. C., & Lam, T. P. (2016). A reliability and validity study for Scolioscan: A radiation-free scoliosis assessment system using 3D ultrasound imaging. *Scoliosis and Spinal Disorders*, *11*(1), 1–15.
25. Sayed, T., Khodaei, M., Hill, D., & Lou, E. (2022). Intra- and inter-rater reliabilities and differences of kyphotic angle measurements on ultrasound images versus radiographs for children with adolescent idiopathic scoliosis: a preliminary study. *Spine Deformity*, *10*(3), 501–507.
26. Daniel, E. S., Lee, R. Y., & Williams, J. M. (2022). The reliability of video fluoroscopy, ultrasound imaging, magnetic resonance imaging and radiography for measurements of lumbar spine segmental range of motion in-vivo: A review. *Journal of Back and Musculoskeletal Rehabilitation*. <https://doi.org/10.3233/BMR-210285>

Publisher's Note Springer Nature remains neutral with regard to jurisdictional claims in published maps and institutional affiliations.

Springer Nature or its licensor (e.g. a society or other partner) holds exclusive rights to this article under a publishing agreement with the author(s) or other rightsholder(s); author self-archiving of the accepted manuscript version of this article is solely governed by the terms of such publishing agreement and applicable law.